Engineering Innovations
ISSN: 2813-1002, Vol. 13, pp 13-23
doi:10.4028/p-DHpNP1

Submitted: 2024-02-27
Accepted: 2024-03-07
Online: 2025-02-06

Optimizing Power Quality in Hybrid Renewable Energy Systems through Advanced Intelligent Control Techniques

Hitesh Kumawat[1,a*], Prerna Tundwal[2,b], Vikramaditya Dave[3,]

[1,2]Ph.D Scholar, Electrical Engineering Department, College of Technology and Engineering MPUAT, Udaipur, 313001, India

[3]Associate Professor, Electrical Engineering Department, College of Technology and Engineering MPUAT, Udaipur, 313001, India

[a*]hiteshkumawat64@gmail.com, [b]sainiprera.97@gmail.com, [c]vdaditya1000@gmail.com

Keywords: PV, Power Quality, WECS, standalone hybrid system, Battery, ANN.

Abstract. The ability of hybrid renewable energy systems (HRES) to combine the advantages of several renewable energy sources has attracted a lot of attention. The intermittent nature of renewable energy sources, such wind and solar power, can make it difficult to keep the grid's power quality constant. Advanced intelligent control strategies are presented in this work with the goal of improving power quality in HRES. In order to reduce power quality difficulties, the research suggests a multidimensional approach that combines the capabilities of advanced control algorithms, intelligent decision-making, and predictive analytics. The main goal is to solve typical issues in HRES, such as harmonic distortions, voltage fluctuations and frequency variations. Proactive system management is made possible by the control approach, which forecasts renewable energy generation trends using machine learning techniques. In addition, real-time monitoring and control systems are included to enable prompt responses to modifications in the power generating mix. The HRES guarantees smooth integration and interaction by utilizing sophisticated hardware and software components to achieve these control mechanisms. This paper presents the results of an extensive simulation research that shows how well the suggested intelligent control solutions mitigate problems with power quality. The results show that the grid's frequency regulation, harmonic distortions, and voltage stability have all significantly improved.

1. Introduction

The integration of various renewable resources has resulted from the progression toward sustainable energy sources, making hybrid renewable energy systems (HRES) a key component of modern power generation. However, the unstable and irregular nature of renewable energy sources makes it difficult to consistently provide high-quality power. To overcome this challenge, advanced control schemes that preserve optimal power quality while quickly adjusting to HRES changes must be developed [1]. For renewable energy systems to be widely adopted, the provision of consistent and dependable power quality is essential. Important aspects of power quality that directly affect the effectiveness and dependability of energy transmission are voltage stability, frequency regulation, and harmonics elimination. But because renewable energy is dynamic, traditional control strategies frequently cannot keep up, which leads to poor power quality and unstable grids [2]. Using cutting edge technologies like artificial intelligence, machine learning, and sophisticated control algorithms, this research aims to investigate and suggest enhanced intelligent control solutions tailored for HRES. By managing energy flow dynamically, reducing disruptions, and enabling the smooth integration of various renewable sources, these strategies aim to improve power quality within HRES [3]. The use of intelligent control techniques aims to address technical challenges while simultaneously meeting the growing need for flexible and durable energy systems. This research aims to improve the performance of HRES by utilizing intelligent control, providing the way for improved sustainability, efficiency, and dependability in the use of renewable energy sources [4]. The application of various intelligent control strategies to improve power quality inside HRES will be thoroughly examined in this study. By means of simulations and practical case studies, our

objective is to demonstrate the effectiveness and potential of these approaches in ensuring stable and superior power distribution, accelerating the shift towards a more sustainable and reliable energy environment [5].

2. Description of Proposed Hybrid System

The new control method for features that improve power quality is created with the proposed standalone hybrid microgrid system. If the battery's charging current is excessive, the supercapacitor will enter the charging mode. In addition, the battery will be discharged initially. If the battery's discharging current is excessive, the supercapacitor will enter the discharging mode in order to meet the load's power requirement. The three phase fully controlled inverter bridge's gate pulse is produced by an FLC-based controller. The AC and DC busses are connected via the fuzzy-based regulated inverter. To produce three phase AC voltage of the necessary amplitude, frequency, and low harmonic content, the LC filter circuit is used. Fig. 1 displays the block diagram of the newly designed novel control technique for a standalone hybrid wind solar PV microgrid system [6].
To keep the load voltage constant, a dynamic voltage restorer (DVR) is used at the load side. The improvement of microgrid power quality is the main objective of the suggested control approach. The voltage source inverter with FLC based capability can effectively minimize harmonics and prevent them from entering the load/grid side [7].

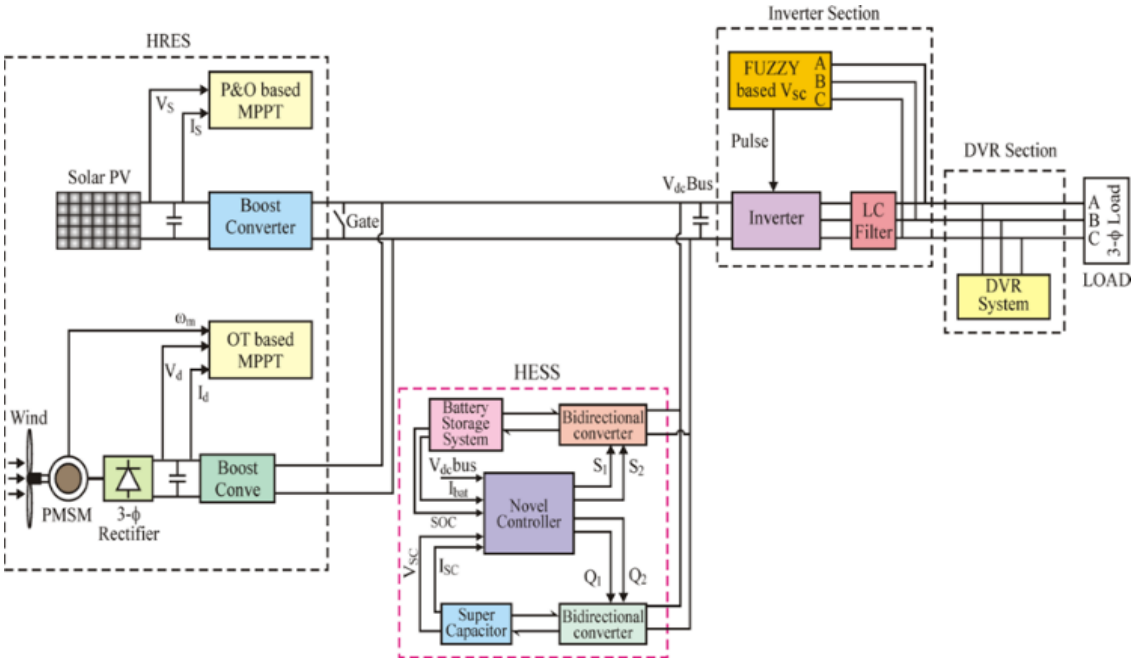

Fig. 1 Block Diagram of the Newly Designed Novel Control Technique for a Standalone Hybrid Wind Solar PV Microgrid System [8]

In order to reduce voltage sag/swell, imbalance, and enhance system power quality, the DVR is linked at the PCC. With an injecting transformer, a voltage source inverter provides the appropriate voltage injection to make up for the difference between supply and load side feeders F1 and F2, respectively. The undesirable harmonic components are suppressed using the LC filter circuit. The connected load receives three-phase electricity from the AC bus.

3. Control of System Components

Fig. 2 displays the block diagram for the suggested ANN-based control technique for hybrid storage management.

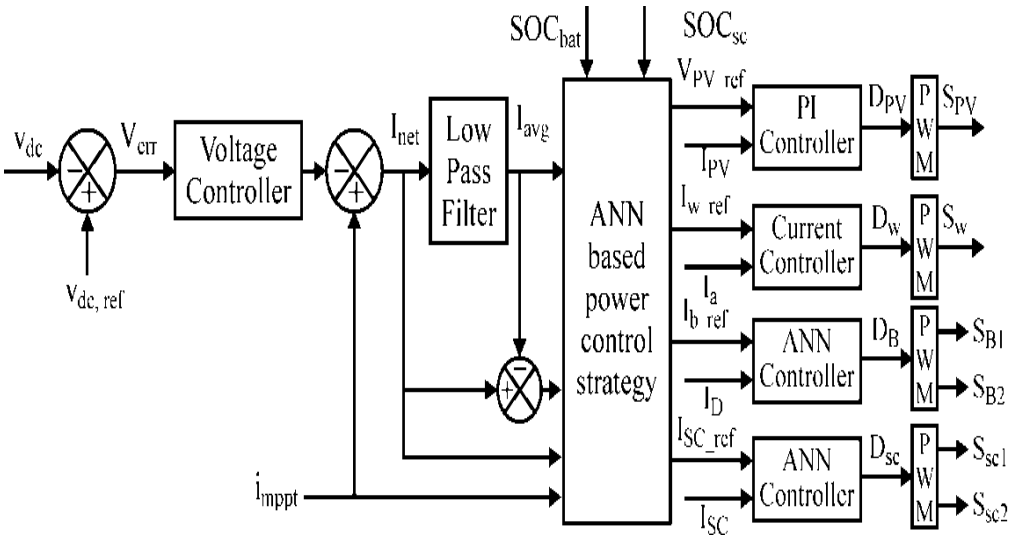

Fig. 2 Block Diagram for the Suggested ANN-Based Control Technique [9]

The following control schemes are suggested for the microgrid in order to efficiently manage the hybrid energy storage system.
(i) To increase the suggested microgrid's efficiency, an MPPT control method is created to capture the most electricity possible from the hybrid solar and wind system [10].
(ii) The excess power is stored in HESS in the following ways when the hybrid system's power generation exceeds the load requirement. When the battery's charging current is low, bi-directional converter 1 uses the excess power produced by RESs to charge the battery. Part of the excess power produced will charge the supercapacitor via directional converter 2 when the charging current exceeds the predetermined threshold value. Both of the converters will function in buck mode under these circumstances [10,11].
(iii) The HESS supplies load power when the hybrid system's power generation is less than the demand for the load. The battery supplies the shortfall in power in the following ways. When the battery's discharge current is low, the battery uses the bi-directional converter 1 to transfer the power difference to the DC bus in order to meet the load's high power requirement. Part of the shortfall power will be supplied by the supercapacitor to the DC bus via bi-directional converter 2 when the battery's discharge current exceeds the predetermined threshold value. Both of the converters will run in boost mode under these circumstances [10,11].

4. Simulation Results and Discussion

The setup shows how different components are displayed in the MATLAB/Simulink program, together with Simulink blocks and the necessary interface circuits for improved hybrid microgrid power generation.
To provide electricity to an off-grid community, a hybrid PV-wind system coupled with a hybrid energy storage system (HESS) is the suggested microgrid. MG consists of the following: a bidirectional (DC-DC) converter connects the PV system; an ANN-based controller controls the HESS system; and WECS is connected via a boost converter using the optimal torque (OT) based MPPT technique. These converters are connected to the 640 V common dc link. The AC loads are powered by the fuzzy based VSC regulated inverter. In order to reduce imbalance, improve system power quality, and minimize voltage sag/swell, the DVR is linked at the PCC. Through the use of an injecting transformer and a voltage source inverter, the difference between supply and load side feeders F1 and F2, respectively, is compensated for. The circuit of the LC filter is used to suppress the undesirable harmonic components. The battery gets charged initially when there is enough wind and solar power to create more energy than the load requires. In the event that the battery's discharging current is excessive, the supercapacitor will enter the discharging mode in order to meet

the load's power requirement. In the event that the battery's charging current is excessive, the supercapacitor will enter the charging mode in addition to being initially drained [12].

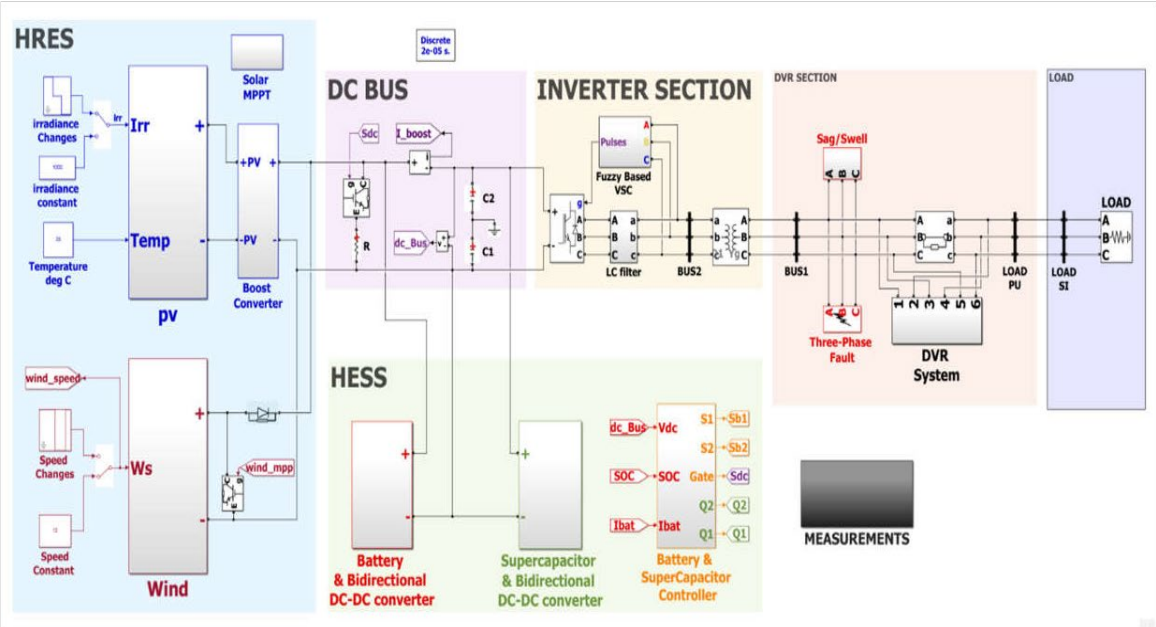

Fig. 3 MATLAB/Simulink Implementation of Dynamic Model for Hybrid Solar PV Wind Microgrid [12]

This system displays many Simulink experiments created aimed at the potential uses of a model of an effective control strategy for hybrid generation systems in stand-alone power generation mode. Studies comparing ANN-based DVRs to traditional dynamic voltage restorers are presented. Where in the dynamic performance of an artificial neural network (ANN)-based DVR is examined under several fault scenarios, such as symmetrical, asymmetrical, and sag and swell situations [13].

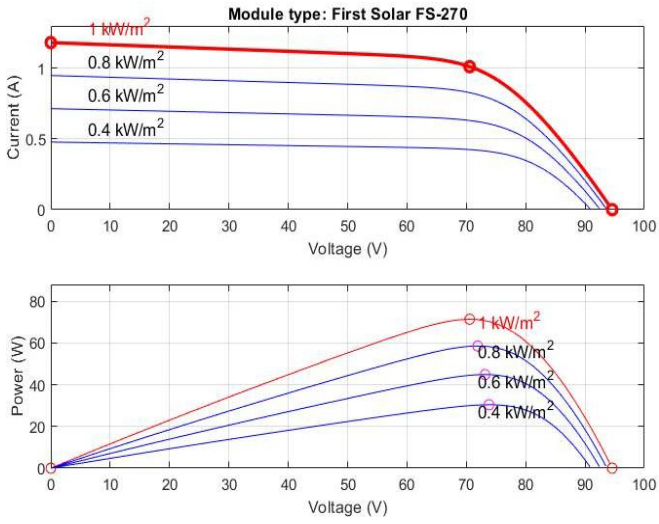

Fig. 4 V-I and P-V Characteristics of Single Module at 1000, 800, 600 and 400W/m2 Irradiances (T=25ºC) [13]

Figure 4 above shows the I-V and P-V characteristics for a single PV module at various irradiation levels. At a module temperature of 298 K (25 ºC), the characteristics are provided for various irradiance levels, namely at 1000W/m², 800W/m², 600W/m², and 400W/m².

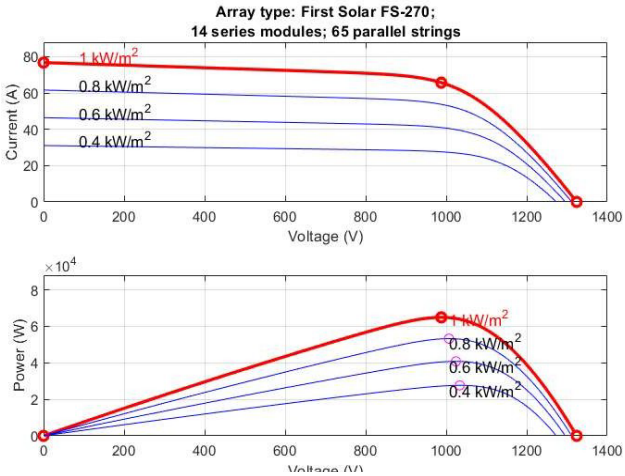

Fig. 5 V-I and P-V Characteristics of PV Array at 1000, 800, 600 and 400W/m2 Irradiances (T=25ºC) [13]

The I-V and P-V characteristics of a PV array system with 65 strings connected in parallel and 14 modules connected in series are displayed in Fig. 5. The PV array's peak output power at 1000 W/m² and 25 ºC is 62.9kW.

At a temperature of 298 K (25 ºC), characteristics are presented for various irradiance levels of 1000 W/m², 800 W/m², 600 W/m², and 400 W/m².

Case 1. **Simulation Response During Asymmetrical Fault at Constant Load With Varying Wind Speed and Varying Irradiance**

simulation results for Line-to-line fault-

The stair-case profile of irradiance is utilized over the whole simulation period, as fig. 6 illustrates. The irradiance varies over time from 400 w/m2 to 600 w/m2, 800 w/m2, and 1000 w/m2, respectively, over the intervals t=0 to t=0.6, t=0.6 to t=1.2, t=1.2 to t=1.8, and t=1.8 to t=2.5. Throughout the simulation, the load and temperature remained constant [14,15].

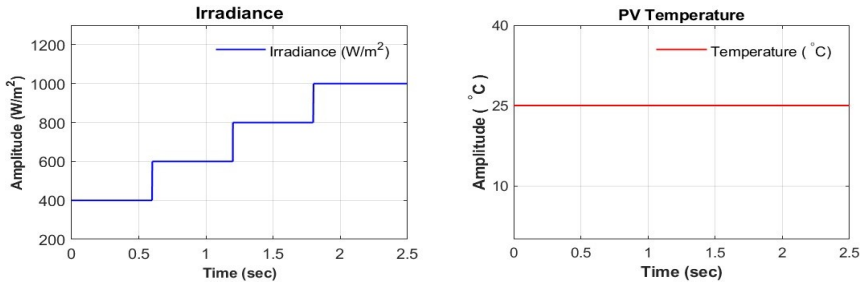

Fig. 6 Waveform of Irradiance and Temp Where Constant Load, Variable Irradiance, Variable Wind Speed [14,15,16]

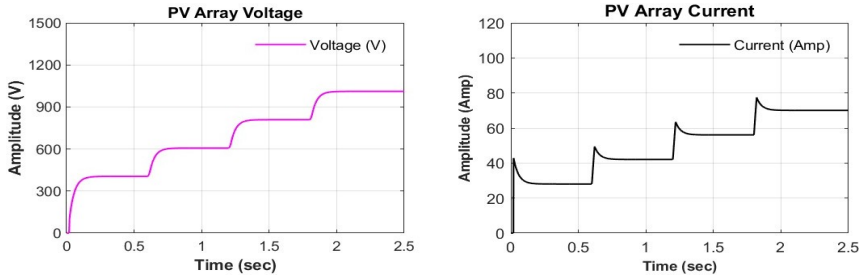

Fig. 7 Waveform of Photovoltaic Voltage and Photovoltaic Current Where Constant Load, Variable Irradiance, Variable Wind Speed [14,15,16]

As shown in fig 7, PV array current varies from 28A to 42A to 56A to 70A during time durations of t=0 to t=0.6sec, t=0.6 to t=1.2sec, t=1.2 to t=1.8sec, and t=1.8 to t=2.5sec, respectively. PV array voltages vary from 404.6V to 606.8V to 809V to 1011V [14].

As shown in fig. 8, the supplied wind speed fluctuates during the simulation. The PMSG rotor speed fluctuates in accordance with the variations in the input wind speed, which ranges from 12 m/s to 8 m/s to 9 m/s to 10 m/s. Specifically, it changes from 1930 rpm to 1120 rpm to 1311 rpm to 1517 rpm throughout the course of t=0 to t=0.8sec, t=0.8 to t=1.4sec, t=1.4 to t=2.1sec, and t=2.1 to t=2.5sec, respectively [14,15].

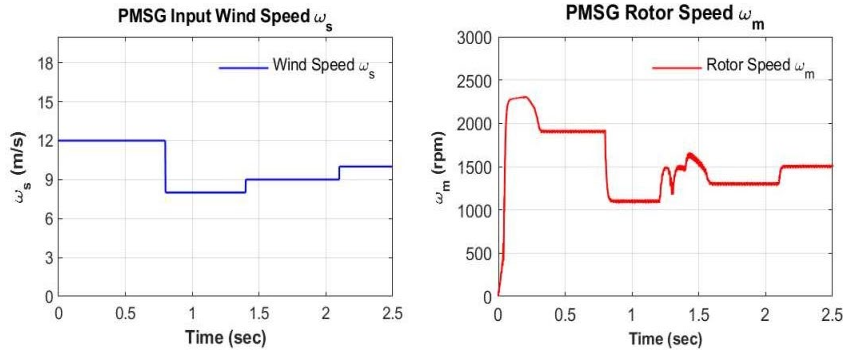

Fig. 8 Waveform of Input Wind Speed and Rotor Speed Where Constant Load, Variable Irradiance, Variable Wind Speed [14,15,16]

As shown in fig 9, The PMSG Electromagnetic & Mechanical Torque changes from 344N-m to 230N-m to 255.6N-m to 288.2N-m within time durations of: t=0 to t=0.8sec, t=0.8 to t=1.4sec, t=1.4 to t=2.1sec, and t=2.1 to t=2.5sec, respectively. The PMSG output power varies from 40800W to 16380W to 20520W to 26670W [14].

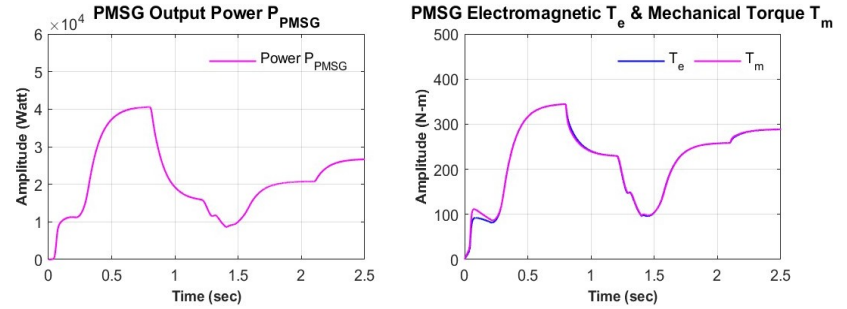

Fig. 9 Waveform of PMSG Output Power and PMSG Te and Tm Where Constant Load, Variable Irradiance, Variable Wind Speed [14,15,16]

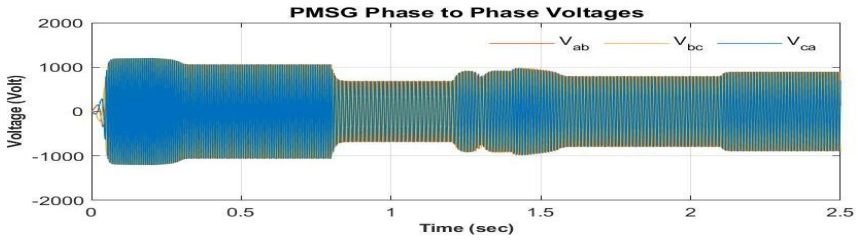

Fig. 10 Waveform of PMSG ph-to-ph Voltage Vph Where Constant Load, Variable Irradiance, Variable Wind Speed [14,15,16]

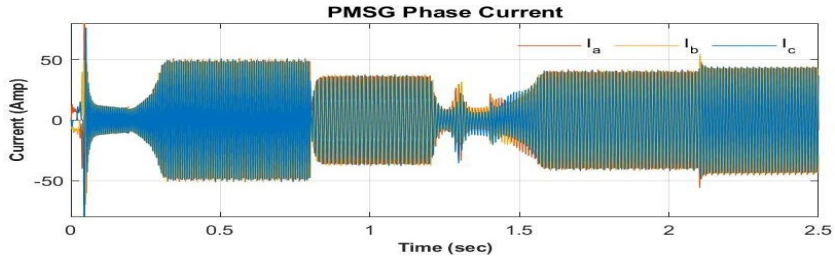

Fig. 11 Waveform of PMSG ph Current Iph Where Constant Load, Variable Irradiance, Variable Wind Speed [14,15,16]

As shown in fig. 10 & fig. 11 PMSG phase current and phase-to-phase voltage fluctuate in response to changes in the input wind speed. Additionally, we can see that there are certain distortions in the PMSG phase voltage and phase current waveforms when a line-to-line fault occurs in the system between time t=1.2 and t=1.3 seconds [14].
In Fig. 12 the output power of the PMSG (in KW) is displayed compared to changing wind speeds.

Fig. 12 Waveform of PMSG Output Power and Wind Speed Where Constant Load, Variable Irradiance, Variable Wind Speed [14,15,16]

According to fig. 13 Phase-to-phase voltage on the generator side remains constant until time t=1.2 seconds, at which point a line-to-line fault causes a slight fall in voltage. The system subsequently stabilizes at t=1.3 seconds, at which point the voltage returns to its initial constant level [14].

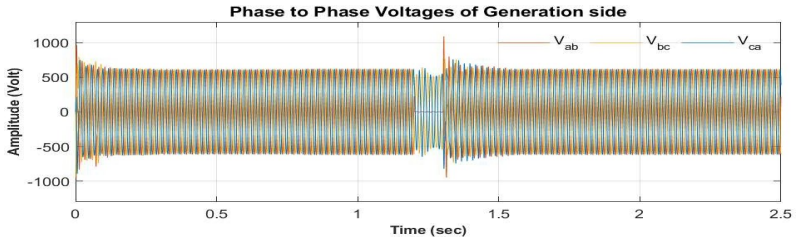

Fig. 13 Waveform of ph-to-ph Voltages of Generation Side Where Constant Load, Variable Irradiance, Variable Wind Speed [14,15,16]

According to fig. 14 Phase-to-phase current on the generating side remains constant until t=1.2 seconds, at which point it increases as a result of a line-to-line fault. The system then stabilizes at t=1.3 seconds, at which point the current returns to its initial value [14].

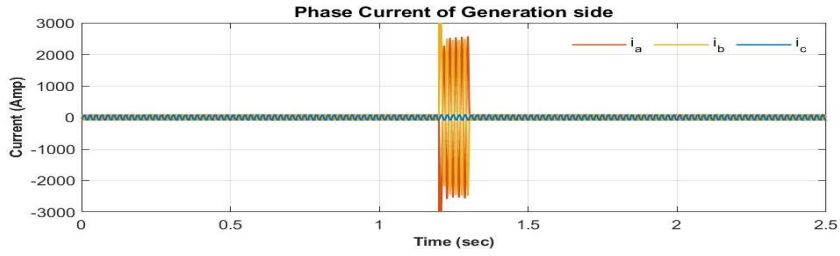

Fig. 14 Waveform of ph Current of Generation Side Where Constant Load, Variable Irradiance, Variable Wind Speed [14,15,16]

Because the network's ANN-tuned DVR compensates for distortions in the generation side voltage to load side voltage, the phase-to-phase voltage of the load remains constant throughout the simulation period, even when the system experiences a line-to-line fault (fig. 15). This is also visible in the zoomed-in window for the phase voltage of the load in fig. 16 [14].

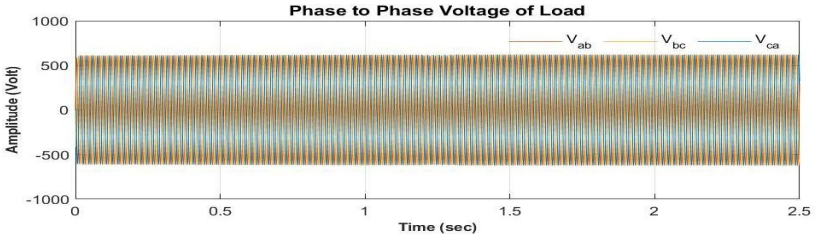

Fig. 15 Waveform of ph-to-ph Voltage of Load Where Constant Load, Variable Irradiance, Variable Wind Speed [14,15,16]

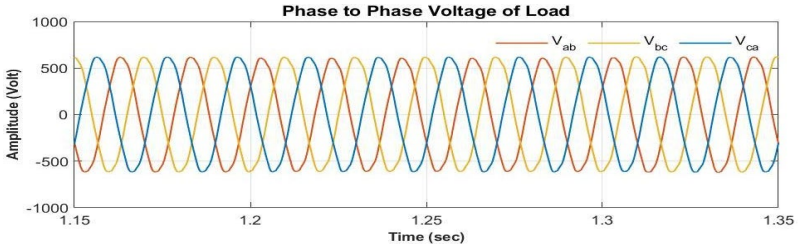

Fig. 16 Waveform of ph-to-ph Voltage of Load L-to-L Fault Where Constant Load, Variable Irradiance, Variable Wind Speed [14,15,16]

Figure 17 shows that the load's phase current remains constant at 92A. However, there is a minor distortion from time t=1.2 sec to t=1.3 sec, which is clearly visible in the zoomed-in window shown in Figure 18 [14].

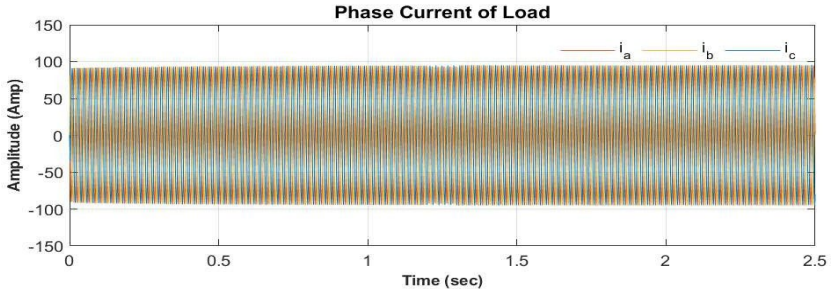

Fig. 17 Waveform of ph Current of Load Where Constant Load, Variable Irradiance, Variable Wind Speed [14,15,16]

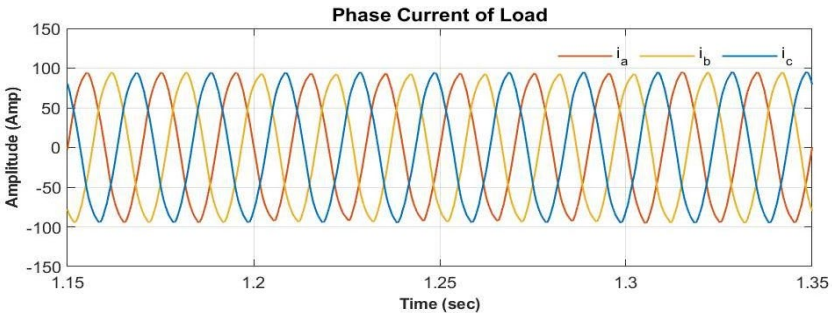

Fig. 18 Waveform of ph Current of Load L-to-L Fault Where Constant Load, Variable Irradiance, Variable Wind Speed [14,15,16]

As shown in fig. 19 throughout the simulation, the load's RMS voltage and RMS current stay constant and only slightly alter during a line-to-line fault [15].

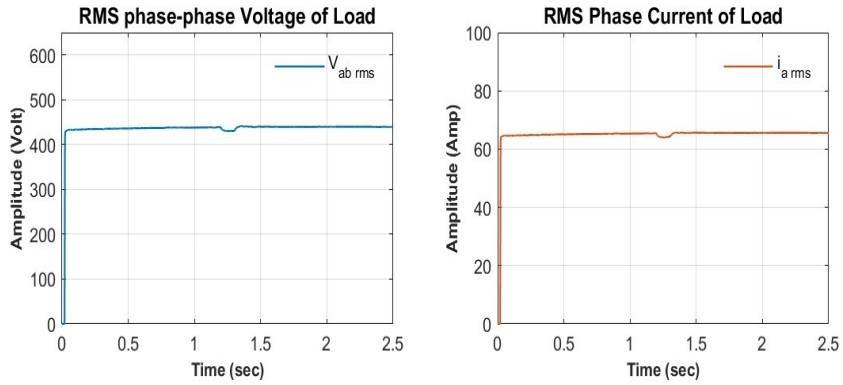

Fig. 19 Waveform of ph-to-ph RMS Voltage of Load and RMS ph Current of Load Where Constant Load, Variable Irradiance, Variable Wind Speed [14,15,16]

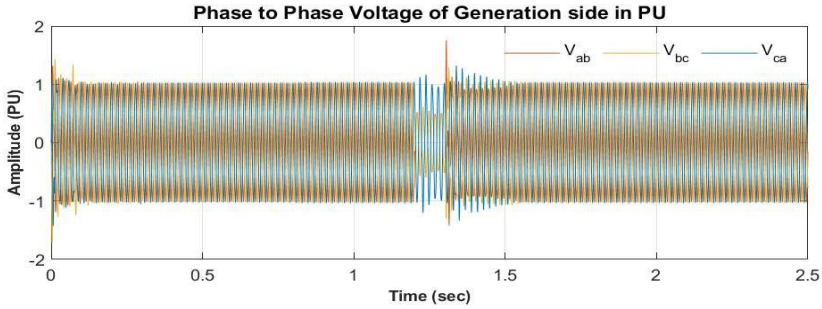

Fig. 20 Waveform of ph-to-ph Voltage of Generation Side in PU Where Constant Load, Variable Irradiance, Variable Wind Speed [14,15,16]

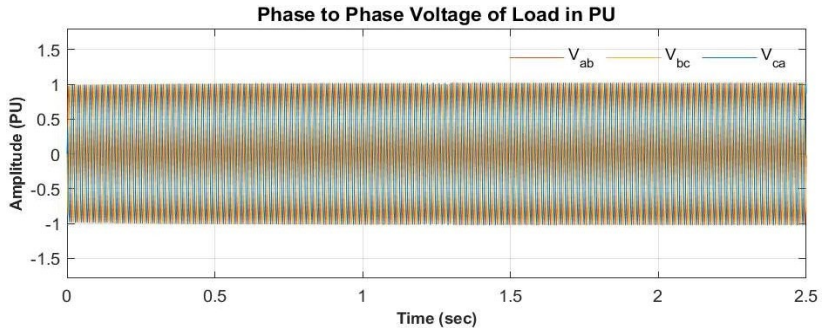

Fig. 21 Waveform of ph-to-ph Voltage of Load Side in PU Where Constant Load, Variable Irradiance, Variable Wind Speed [14,15,16]

Figure 20 clearly illustrates the distortions caused by a line-to-line fault, which resulted in a decrease in the phase-to-phase voltage of the generation side. However, Figure 21 illustrates how an asymmetrical fault does not affect the phase-to-phase voltage on the load side because the system uses an ANN-tuned DVR to isolate the load when a line-to-line fault occurs [14].

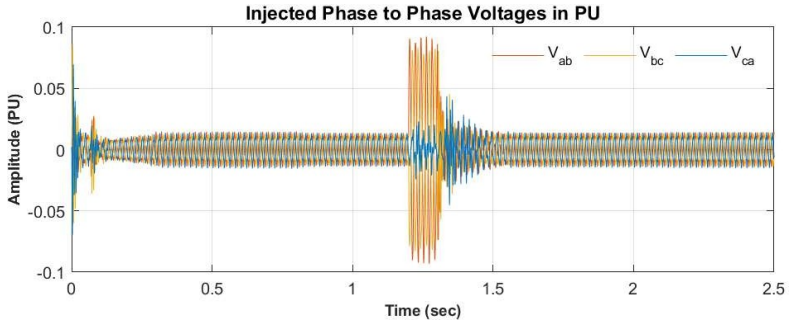

Fig. 22 Waveform of Injected ph-to-ph Voltage in PU Where Constant Load, Variable Irradiance, Variable Wind Speed [14,15,16]

Figure 22 makes it evident that, in the event of a malfunction, an ANN-tuned DVR will inject phase voltages into the load while isolating it from the generator side, ensuring a continuous and distortion-free voltage supply to the load [14].
Figures 23 and 24 display the phase current of the load side and the phase current of the generator side for each unit system [14].

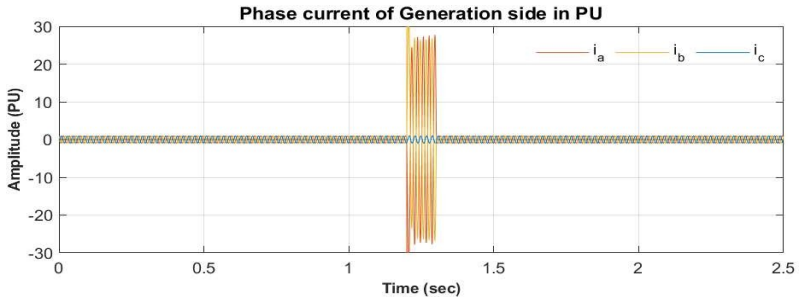

Fig. 23 Waveform of ph Current of Generation Side in PU Where Constant Load, Variable Irradiance, Variable Wind Speed [14,15,16]

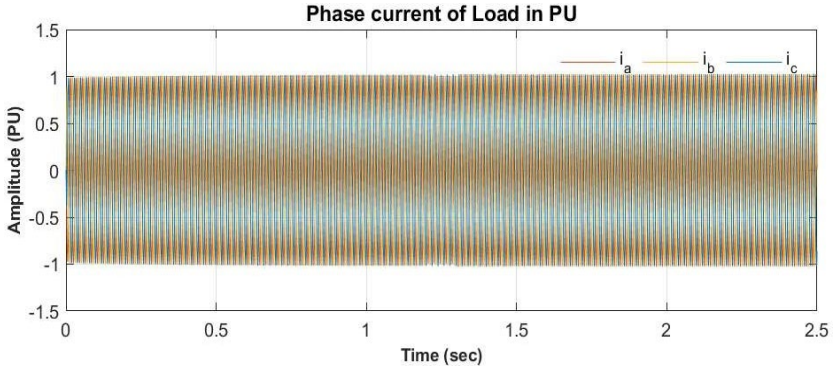

Fig. 24 Waveform of ph Current of Load Side in PU Where Constant Load, Variable Irradiance, Variable Wind Speed [14,15,16]

5. Conclusion

In conclusion, a critical approach to resolving power quality issues in hybrid renewable energy systems is the incorporation of sophisticated intelligent control mechanisms. This study highlights a notable improvement in power quality indicators, including harmonic mitigation, frequency stability, and voltage regulation, by combining renewable energy sources, such as solar and wind power, with creative control algorithms. Intelligent controls' adaptable nature allows for dynamic response to variations, guaranteeing maximum performance in a range of scenarios. In addition to paving the way for a dependable and stable power supply, these solutions' effective execution and proven effectiveness also support the more general goals of sustainability and effective use of renewable resources. Further advancements and real-world implementations of these strategies hold immense promise in revolutionizing the future of energy systems, fostering a sustainable, resilient, and high-quality power infrastructure.

References

[1] A. Alexander, M. Thathan, Modelling and analysis of modular multilevel converter for solar photovoltaic applications to improve power quality. IET renewable power Generation. 2015 Jan;9(1):78-88.

[2] S. Arezki, M. Boudour, Improvement of power quality for hybrid PV-FC power supply system. In2014 16th International Power Electronics and Motion Control Conference and Exposition 2014 Sep 21 (pp. 725-730). IEEE.

[3] PG. Arul, VK. Ramachandaramurthy, RK. Rajkumar, Control strategies for a hybrid renewable energy system: A review. Renewable and sustainable energy reviews. 2015 Feb 1;42:597-608.

[4] A. Chauhan, RP. Saini, A review on Integrated Renewable Energy System based power generation for stand-alone applications: Configurations, storage options, sizing methodologies and control. Renewable and Sustainable Energy Reviews. 2014 Oct 1;38:99-120.

[5] F. Chishti, S. Murshid, B. Singh, LMMN-based adaptive control for power quality improvement of grid intertie wind–PV system. IEEE Transactions on Industrial Informatics. 2019 Feb 3;15(9):4900-12.

[6] W. Jing, C. Hung Lai, SH. Wong, ML. Wong, Battery-supercapacitor hybrid energy storage system in standalone DC microgrids: areview. IET Renewable Power Generation. 2017 Mar;11(4):461-9.

[7] K. Zeb, SU. Islam, I. Khan, W. Uddin, M. Ishfaq, TD. Busarello, SM. Muyeen, I. Ahmad, HJ. Kim, Faults and Fault Ride Through strategies for grid-connected photovoltaic system: A comprehensive review. Renewable and Sustainable Energy Reviews. 2022 Apr 1;158:112125.

[8] R. Sedaghati, MR. Shakarami, A novel control strategy and power management of hybrid PV/FC/SC/battery renewable power system-based grid-connected microgrid. Sustainable Cities and Society. 2019 Jan 1;44:830-43.

[9] M. Amir, ANN Based Approach for the Estimation and Enhancement of Power Transfer Capability. In2019 International Conference on Power Electronics, Control and Automation (ICPECA) 2019 Nov 16 (pp. 1-6). IEEE.

[10] TC. Ou, CM. Hong, Dynamic operation and control of microgrid hybrid power systems. Energy. 2014 Mar 1;66:314-23.

[11] LW. Chong, YW. Wong, RK. Rajkumar, D. Isa, Hybrid energy storage systems and control strategies for stand-alone renewable energy power systems. Renewable and sustainable energy reviews. 2016 Dec 1;66:174-89.

[12] G. Bayrak, M. Cebeci, Grid connected fuel cell and PV hybrid power generating system design with Matlab Simulink. International journal of hydrogen energy. 2014 May 27; 39 (16): 8803-12.

[13] P. Bajpai, V. Dash, Hybrid renewable energy systems for power generation in stand-alone applications: A review. Renewable and Sustainable Energy Reviews. 2012 Jun 1;16(5):2926-39.

[14] H. Kumawat, R. Jangid, Using AI Techniques to Improve the Power Quality of Standalone Hybrid Renewable Energy Systems. InCrafting a Sustainable Future Through Education and Sustainable Development 2023 (pp. 219-250). IGI Global.

[15] H. Kumawat, P. Tundwal, V. Dave, Intelligent Control Strategies for Enhancing Power Quality in Hybrid Renewable Energy System for Agricultural Applications. In2023 IEEE World Conference on Applied Intelligence and Computing (AIC) 2023 Jul 29 (pp. 26-32). IEEE.

[16] H. Kumawat, P. Tundwal and V. Dave, "Artificial Intelligence-Enabled Fault Detection and Diagnosis for Improved Power Quality in Hybrid Renewable Energy Systems," *2023 3rd International Conference on Advancement in Electronics & Communication Engineering (AECE)*, GHAZIABAD, India, 2023, pp. 480-485,IEEE.